Accepted Manuscript

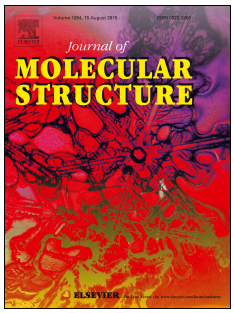

Design and synthesis of a novel mPGES-1 lead inhibitor guided by 3D-QSAR CoMFA

Mohd Fadhlizil Fasihi Mohd Aluwi, Kamal Rullah, Andreas Koeberle, Oliver Werz, Nur Sakinah Abdul Razak, Leong Sze Wei, Fatimah Salim, Nor Hadiani Ismail, Ibrahim Jantan, Lam Kok Wai

PII: S0022-2860(19)30838-5

DOI: https://doi.org/10.1016/j.molstruc.2019.07.004

Reference: MOLSTR 26757

To appear in: *Journal of Molecular Structure*

Received Date: 26 February 2018

Revised Date: 30 April 2019

Accepted Date: 1 July 2019

Please cite this article as: M.F. Fasihi Mohd Aluwi, K. Rullah, A. Koeberle, O. Werz, N.S. Abdul Razak, L.S. Wei, F. Salim, N.H. Ismail, I. Jantan, L.K. Wai, Design and synthesis of a novel mPGES-1 lead inhibitor guided by 3D-QSAR CoMFA, *Journal of Molecular Structure* (2019), doi: https://doi.org/10.1016/j.molstruc.2019.07.004.

Graphical Abstract

To create your abstract, type over the instructions in the template box below.
Fonts or abstract dimensions should not be changed or altered.

Design and synthesis of a novel mPGES-1 lead inhibitor guided by 3D-QSAR CoMFA

Leave this area blank for abstract info.

Mohd Fadhlizil Fasihi Mohd Aluwi[a,*] , Kamal Rullah[b] , Andreas Koeberle[c] , Oliver Werz[c] , Nur Sakinah Abdul Razak[d], Leong Sze Wei[e] , Fatimah Salim[f], Nor Hadiani Ismail[f] , Ibrahim Jantan[g] , Lam Kok Wai[d,*]

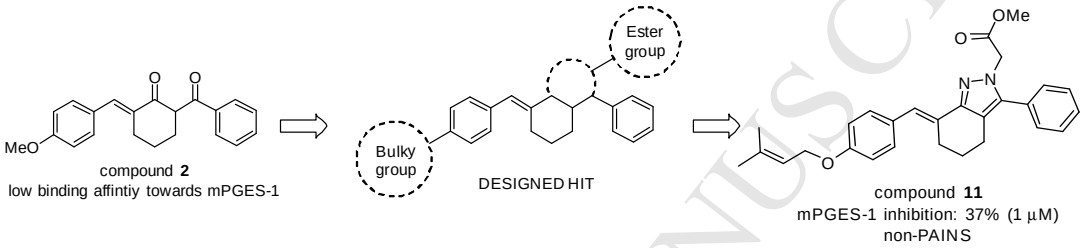

ELSEVIER

Journal of Molecular Structure
journal homepage: www.elsevier.com

Design and synthesis of a novel mPGES-1 lead inhibitor guided by 3D-QSAR CoMFA

Mohd Fadhlizil Fasihi Mohd Aluwi[a,*] , Kamal Rullah[b] , Andreas Koeberle[c] , Oliver Werz[c] , Nur Sakinah Abdul Razak[d], Leong Sze Wei[e] , Fatimah Salim[f], Nor Hadiani Ismail[f] , Ibrahim Jantan[g] , Lam Kok Wai[d,*]

[a]*Faculty of Industrial Science & Technology, Universiti Malaysia Pahang, Lebuhraya Tun Razak, 26300, Gambang, Pahang, Malaysia*
[b]*Department of Pharmaceutical Chemistry, Kuliyyah of Pharmacy, International Islamic University Malaysia, Bandar Indera Mahkota, 25200, Kuantan, Pahang, Malaysia*
[c]*Department of Pharmaceutical/Medicinal Chemistry, Institute of Pharmacy, Friedrich-Schiller-University Jena, 07743 Jena, Germany*
[d]*Drug and Herbal Research Centre, Faculty of Pharmacy, Universiti Kebangsaan Malaysia, Jalan Raja Muda Abdul Aziz, 50300, Kuala Lumpur, Malaysia*
[e]*Department of Microbiology, Faculty of Biotechnology and Biomolecular Sciences, Universiti Pura Malaysia, 43400, Serdang, Selangor, Malaysia*
[f]*Atta-ur-Rahman Institute for Natural Product Discovery, Universiti Teknologi MARA, Kampus Puncak Alam, 42300, Puncak Alam, Selangor, Malaysia*
[g]*School of Pharmacy, Taylor University Lakeside Campus, No 1, Jalan Taylor's, 47500, Subang Jaya, Selangor Darul Ehsan, Malaysia,*

ARTICLE INFO

Article history:
Received
Revised
Accepted
Available online

Keywords:
3D-QSAR CoMFA
PGE_2
mPGES-1
PAINS

ABSTRACT

The search of novel mPGES-1 inhibitors has recently intensified probably due to the superior safety in comparison to existing anti-inflammatory drugs. Although two mPGES-1 inhibitors have entered clinical trials, none has yet reached the market. In this study, we performed modifications guided by 3D-QSAR CoMFA on **2**, which is an unsymmetrical curcumin derivative with low binding affinity towards mPGES-1. To counter the PAINS properties predicted for **2**, the diketone linker was replaced with a pyrazole ring. On the other hand, both prenyl and carboxylate ester groups were introduced to improve the activity. When tested *in vitro*, **11** suppressed PGE_2 biosynthesis in activated macrophages and showed promising human mPGES-1 inhibition in microsomes of interleukin-1β-stimulated A549 cells. Altogether, **11** has been identified as a potential mPGES-1 inhibitor and could be a promising lead for a novel class of mPGES-1 inhibitors.

Introduction

Microsomal prostaglandin E_2 synthase (mPGES)-1 has garnered an extraordinary amount of interest as a potential therapeutic target for the treatment of inflammation-related diseases. It is a terminal enzyme that is part of the membrane-associated protein (MAPEG) superfamily, which is involved in eicosanoid and glutathione metabolism [1]. In general, this protein family comprises 5-lipoxygenase-activating protein (FLAP), leukotriene C_4 synthase (LTC_4S), and microsomal glutathione transferases (MGST1, MGST2, and MGST3). While mPGES-1 is constitutively expressed in lung, kidney and reproductive organs, it is normally found at lower levels elsewhere in the body although it can be strongly upregulated by inflammatory stimuli such as interleukin-1β [2]. Since mPGES-1 is critical to the production of PGE_2, a proinflammatory signaling molecule found in inflammation conditions, it appears to be an attractive drug target for osteoarthritis, rheumatoid arthritis and cancer. This is further supported by scientific evidences that selective mPGES-1 inhibitors could alleviate the effects of excessive production of PGE_2, which promotes inflammation, fever and pain but also stimulates proliferation, differentiation and angiogenesis [3], without suppressing the biosynthesis of other prostanoids downstream of PGH_2.

Curcumin and its derivatives are known to possess a wide range of biological activities such as anti-inflammatory, anti-tyrosinase and immunomodulatory functions [4-10]. More recently, our group had synthesized a series of unsymmetrical monocarbonyl **1** [11] and dicarbonyl curcumin analogues **2** and demonstrated that they could suppress the PGE_2 production level in both LPS-induced human and murine monocytic cell lines. In spite of this, our efforts to develop the molecules had been hampered by the growing evidences that curcumin and its derivatives might be categorized under pan-assay interference substances (PAINS), which are defined by their ability to show activity across a range of assay platforms and against a range of proteins. Many PAINS, including the Michael acceptor curcumin, function as reactive chemicals rather than discriminating between drugs with defined structure activity relationship. Others give false-positive readouts in a variety of ways such as metal chelation, chemical aggregation, redox

* Corresponding author. Tel.: +603-92897031; e-mail: david_lam@ukm.edu.my (Lam Kok Wai); Tel.: +609-5492399; fasihi@ump.edu.my (Mohd Fadhlizil Fasihi Mohd Aluwi)

activity, compound fluorescence, cysteine oxidation or promiscuous binding. Moreover, curcumin is not suitable for clinical application due to its poor oral availability, low aqueous stability and low circulating concentrations in plasma. Whilst the debate is still actively on-going of whether curcumin and its derivatives are suitable to be developed as drugs, we took the challenge to improving the properties of these molecules. Guided by a structural based drug design approach and CoMFA, we made several rational structural modifications to compound **2** (**Figure 1a**) and tested the target compound on mPGES-1 activity.

Interestingly, a quick glance through the list of some of the mPGES-1 inhibitors found in nature (**Figure 1b**) revealed that each of them comprises at least a prenyl group in their structure. It could be a strong indicator that this functional group might play an important role for the inhibitory activity. In fact, recent reports have shown that curcumin and its prenylated analogues also displayed mPGES-1 inhibition [12, 13]. It is known that the presence of a prenyl group in a small molecule not only enhances lipophilicity but also bestows a strong affinity for biological membranes [14]. Nevertheless, it could improve the pharmacokinetic profile of a given compound leading to a broader range of interesting pharmacological activities.

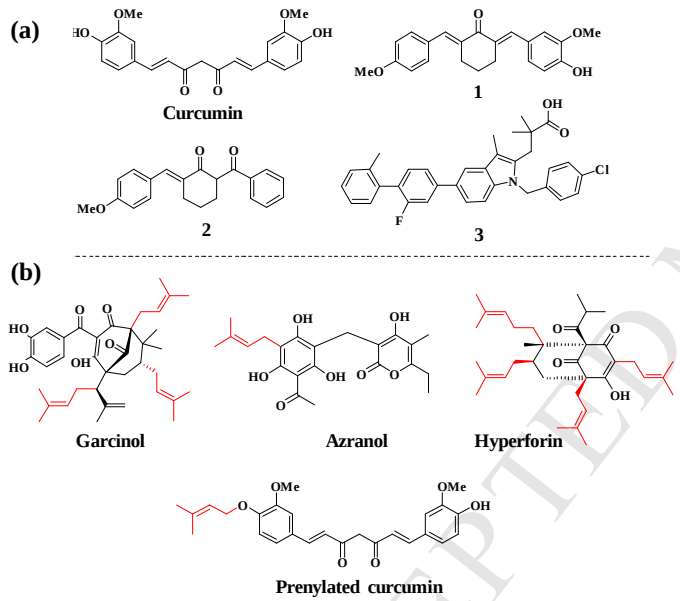

Figure 1. (a) Curcumin, monocarbonyl (**1**) and dicarbonyl (**2**) curcumin derivatives and a MK886 derivative (**3**). **(b)** Selected structures of mPGES-1 inhibitors obtained from natural product isolation and by chemical semi-synthesis.

Results and discussion

3D-QSAR CoMFA

To gain insights into the contour features of mPGES-1 ligand binding site, a set of MK-886 derivatives known to inhibit mPGES-1 activity were retrieved from literature [15] and subjected to docking and 3D-QSAR CoMFA (comparative molecular field analysis) studies. To initiate that, first the mPGES-1 protein crystal structure (PDB ID 4AL1: 1.95 Å) was retrieved from RCSB Protein Data Bank and prepared according to the standard protocol implemented in Discovery Studio 3.1. The reported inhibitors were prepared, minimized and docked to the putative binding site; the complex then underwent *in situ* ligand minimization in a flexible receptor environment to refine the final ligand binding conformation.

CoMFA has been widely used to study steric potential in the form of a Lennard-Jones function and electrostatic potential in the form of a Coulomb function surrounding a set of biologically characterized molecules. Whereas molecular docking has been established as the main approach for recognizing the most likely bioactive conformation of compounds in the receptor binding site. Thus, combining these two methods would result in a more thorough protein-ligand binding interaction analysis. To start with, two different conformational sampling methods were adopted in this study: a structural-based alignment (**method A**) and a docking-based alignment (**method B**) (**Figures 2a** and **b**). For the first method, the top-ranked docked ligand **3** (**Figure 1a**) was initially used to build a hypothesis and predefine the binding conformations of the other compounds. In the latter method, all the compounds were docked to the binding site and their conformations were used without reallignment for further analysis. Both methods accurately predicted the mPGES-1 inhibtory activities of the MK-886 derivatives (**Table 1**). However, only the results from **method B** were discussed here as it has been proven to be more successful in term of predicting the ligand binding mode and describing the contribution of the region of interest surrounding the ligands at the protein target site accurately.

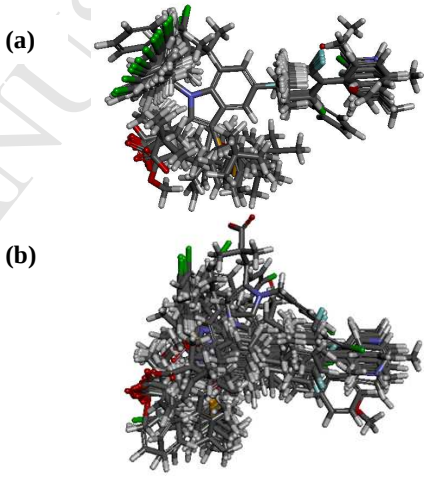

Figure 2: Structural alignment of the MK-886 derivatives by the template-based method according to the core specified by the top-docked conformation of **3**.

In the best model, 29 reported MK-886 derivatives were retrieved, in which 19 compounds were randomly selected as a training set, and the remaining 10 compounds were used as a test set. As stated in **Table 1**, the best model produced was highly predictive with a non-cross-validated correlation coefficient (r^2) of 0.990 and a leave-one-out cross-validated correlation coefficient (q^2) of 0.437 using three principle components. The external predictive ability of the model was further validated with a high q^2 value of 0.759 (**Figure 3**).

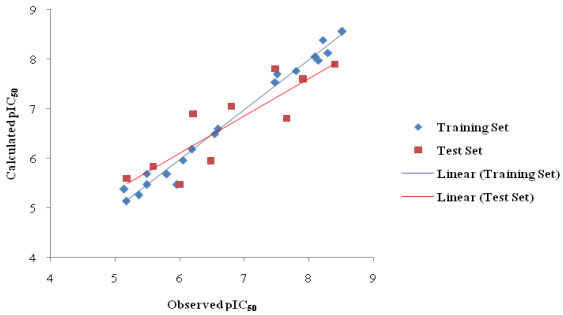

Figure 3: Trend of the observed versus calculated pIC_{50} values of the training-set and test-set compounds.

The steric maps include green contour (**Figure 4a**) that indicates region where the steric bulk groups favor inhibition while the yellow contour (**Figure 4b**) indicates region where steric bulk does not favor activity. Superposition of the contour maps over the binding site of mPGES-1 reveals that the green contours are mainly located at the edge of the shallow groove, which comprises Leu132, Ala133, Gln134, Leu135, Pro136 and Cys137 from helix IV and Val30', Ala31' and Ile32' from helix I' suggesting that sterically bulky substituents are highly favored. On the other hand, the yellow contours can be seen occupying largely the position where cofactor GSH is bound. This suggests that further modifications beyond the phenyl ring at this position is highly unlikely to improve the activity.

The red contour (**Figure 4c**) indicates region where positive electrostatic potential is favorable for activity, and blue contour (**Figure 4d**) indicates region where an increase in negative electrostatic potential enhances activity. Superposition of the contour maps over the binding site of mPGES-1 reveals that blue contours predominantly occupy the region in helix IV suggesting that negative electrostatic functional groups are highly favorable for activity at this position while the red regions are mainly located alongside helix I'. Several blue contour maps are also observed in the positions adjacent to the side chains of Arg38' and Arg52'. The latter residue is known to form an important salt bridge interaction with the carboxylate moiety of a MK-886 derivative important for inhibition of mPGES-1.

Table 1 Statistics of the comparative molecular field analysis models generated using different alignment methods.

Model	Grid Spacing (Å)	Non cross-validation		Leave one out-cross-validation			External predictive *q*-squared	
		r^2 [a]	RMS residual error	q^2 [b]	N [c]	Mean Absolute Error	q^2 [d]	RMS error
Method A (Structural alignment)								
1		0.932	0.3062	0.213	1	0.898	0.828	0.613
2	1.0	-	-	0.201	3	0.897	-	-
3		-	-	0.202	4	0.899	-	-
4		-	-	0.292	3	0.848	-	-
5	1.5	-	-	0.299	4	0.844	-	-
6		1.000	0.0055	0.300	5	0.844	0.793	0.539
7		-	-	0.384	3	0.785	-	-
8	2.0	-	-	0.392	4	0.774	-	-
9		**1.000**	**0.0100**	**0.394**	**5**	**0.772**	**0.869**	**0.510**
Method B (Docking-based alignment)								
10		0.922	0.3276	0.483	1	0.773	0.671	0.591
11	1.0	-	-	0.480	3	0.797	-	-
12		-	-	0.480	4	0.798	-	-
13		0.867	0.4283	0.376	1	0.730	0.695	0.572
14	1.5	-	-	0.361	3	0.771	-	-
15		-	-	0.360	4	0.770	-	-
16		**0.990**	**0.1191**	**0.437**	**3**	**0.688**	**0.759**	**0.501**
17	2.0	-	-	0.436	4	0.691	-	-
18		-	-	0.435	5	0.687	-	-

[a] Non cross-validated correlation coefficient.
[b] Leave one out-cross-validated correlation coefficient.
[c] Optimum number of components obtained from cross-validated PLS analysis.
[d] Correlation coefficient for test set predictions.

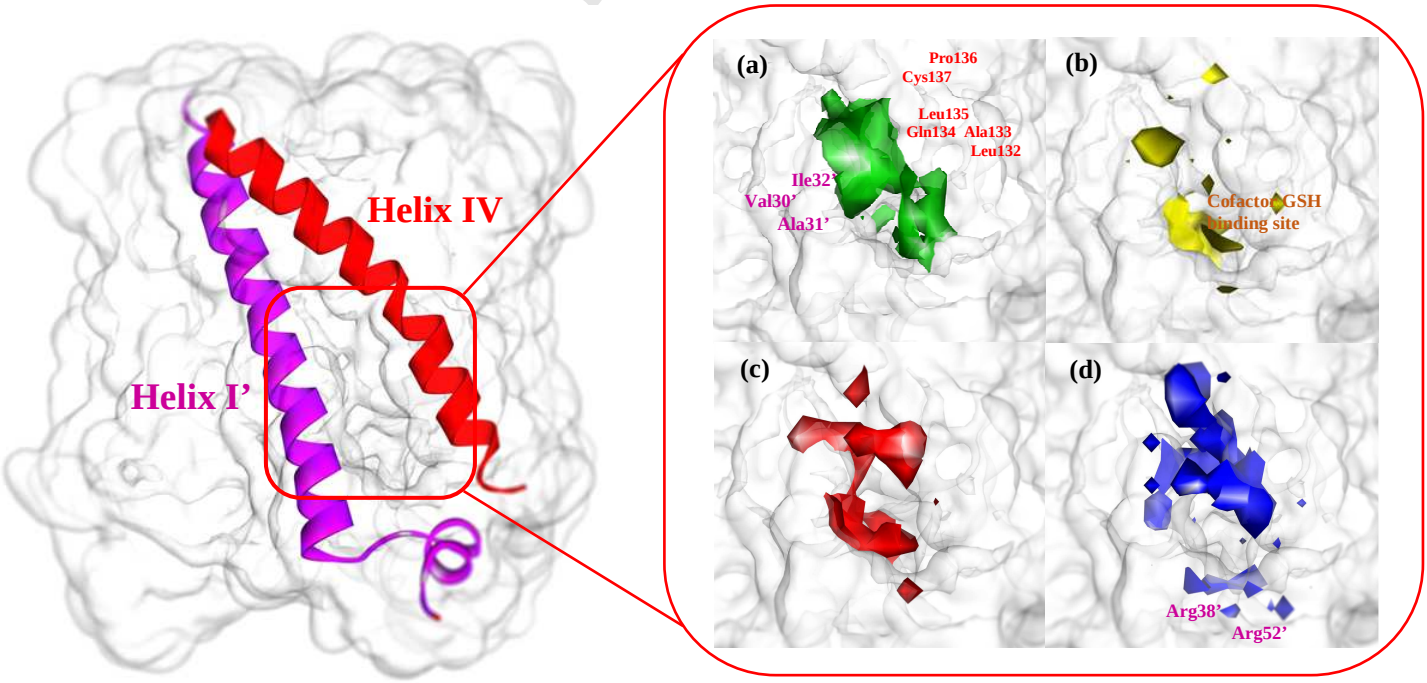

Figure 4: Superposition of the steric ((a) and (b)) and electrostatic ((c) and (d)) contour maps within the putative binding site of human mPGES-1.

Figure 5 depicts the design strategy adopted behind the modifications of compound **2**. Considering that bulky and carboxylic acid moieties critically contribute to the binding affinity of **3** to mPGES-1 as supported in the CoMFA study, we opted to introduce two major functional groups into the designed compound including i) a prenyl group that could occupy the top cavity at the binding groove formed by Leu132, Ala133, Gln134, Leu135, Pro136 and Cys137 from helix IV and Val30', Ala31' and Ile32' from helix I' ii) and a carboxylate ester that could form a salt bridge interaction with Arg38' and Arg52'. With the introduction of these two functional groups, we predict that the inhibitory activity and the binding affinity should be greatly improved.

To initiate the synthesis, the prenyl group was coupled to 4-hydroxybenzaldehyde (**4**) by treatment with 1-chloro-3-methyl-2-butene in the presence of K_2CO_3 in acetone under reflux condition. The desired product **5** was obtained in good yield (80%) (**Scheme 1**) and was used as a building block for the synthesis of **11** as depicted in **Scheme 2**. Cyclohexanone **6** (48 mmol) was reacted with pyrrolidine (48 mmol) in the presence of *p*-toluenesulfonic acid (1 mmol) to afford N-(1-cyclohexenyl)pyrrolidine **7**, an essential enamine intermediate. Next, **7** (1 mmol) was reacted with benzoic anhydride (2 mmol) to obtain the corresponding crude product of 2-benzoylcyclohexanone **8**.

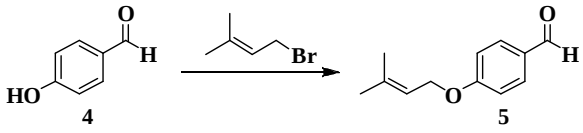

Scheme 1: Reagent and condition: acetone, K_2CO_3, reflux, 20 h.

Subsequent purification by flash chromatography yielded the pure product with a conversion rate of 30-40%. The purified **8** was then reacted with an equivalent amount of B_2O_3 to give the boron complex. The complex was then coupled with the prenylated benzaldehyde **5** in the presence of tributyl borate and *n*-butylamine in ethyl acetate. The reaction was carried out under reflux condition overnight. The crude product was purified using column chromatography to obtain the unsymmetrical dicarbonyl curcumin derivative **9**. Cyclization of the purified **9** was achieved *via* Michael addition by reacting with hydrazine to give pyrazole **10**. Finally, the carboxylate ester group was introduced to the compound *via* *N*-alkylation with methyl 2-bromoacetate in the presence of Cs_2CO_3 in DMF as solvent. The crude product was then purified using column chromatography to obtain the final product **11** in satisfactorily yield (55%) (**Scheme 2**).

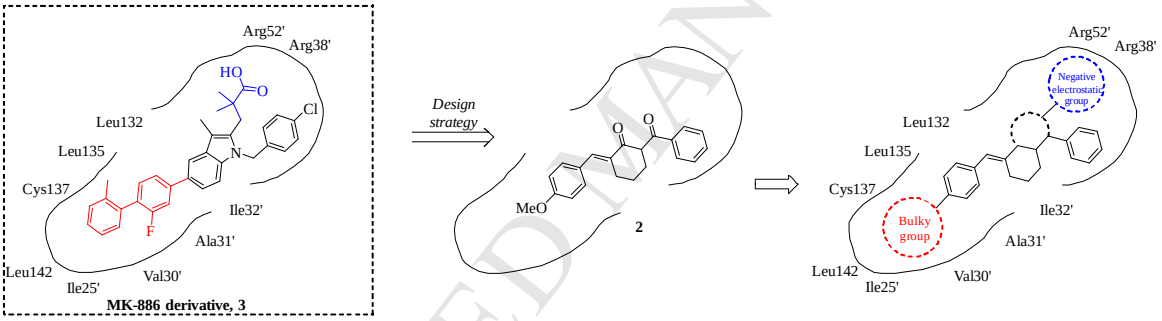

Figure 5: A general design strategy behind the modifications of **2**.

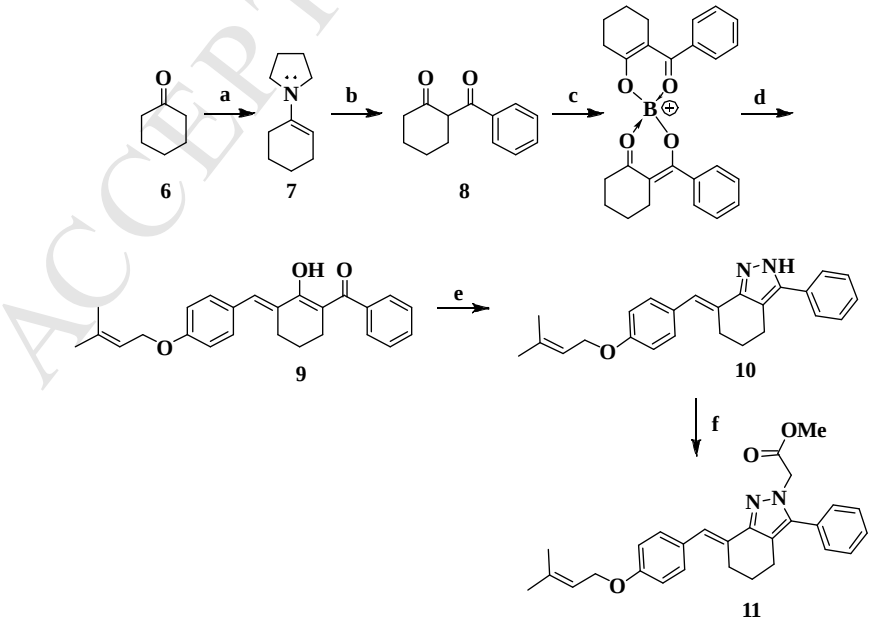

Scheme 2: Reagents and conditions: (a) pyrolidine, *p*-TSOH, toluene, reflux under Dean and Stark apparatus. (ii) Distilled until it reached 108-110°C; (b) benzoic anhydride, toluene, r.t. overnight; (c) B_2O_3, ethyl acetate, refllux, 70°C, 3 h; (d) (i) respective benzaldehyde **5**, tributylborate, 30 min, r.t., (ii) n-butylamine, reflux, 70°C, overnight, (iii) 1 M HCl, reflux, 30 min; e) hydrazine, EtOH, reflux, 1h.; f) methyl 2-bromoacetate, Cs_2CO_3, DMF, r.t.

*Effects of **11** on PGE_2 production level in RAW264.7 macrophages and human cell-free mPGES-1*

To verify whether the designed compound could interfere with mPGES-1 activity, we investigated its effect on mPGES-1-dependent PGE_2 biosynthesis in murine RAW264.7 macrophages. As expected, the compound almost completely suppressed PGE_2 formation (>90%) in LPS-activated macrophages at 25 µM. However, it is known that there is a difference in the mPGES-1 structure between human and murine/rat species. To further confirm whether **11** could act on human mPGES-1, we carefully assessed its inhibitory activity against human cell-free mPGES-1 using microsomes of interleukin-1β-stimulated A549 cells. At 1 µM, **11** was found to inhibit mPGES-1 activity by 37% (**Figure 6**). MK-886 (**Figure S-1**) (10 µM) was used as a reference inhibitor and suppressed the PGE_2 synthesis as expected. Since **11** was designed from the lead compound **2**, which represents a derivative of curcumin, we evaluated its PAINS character using *in silico* tools (FAF-Drug4). Overall, **11** was not categorized as potential PAINS or covalent inhibitor while **2** and curcumin were identified as covalent inhibitors. Thus, **11** might represent a valuable lead for novel mPGES-1 inhibitors that lacks the pan-assay interference activities.

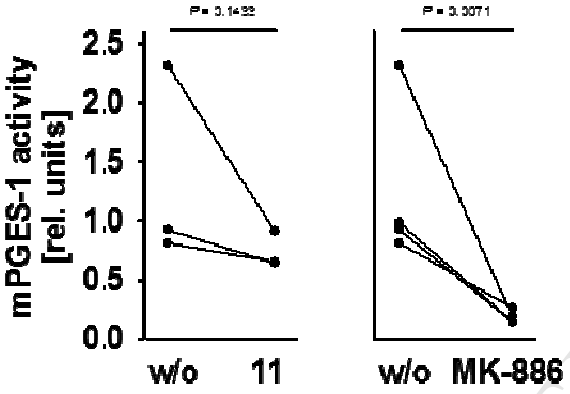

Figure 6: Effect of **11** (1 µM) and the reference inhibitor MK-886 (10 µM) on cell-free mPGES-1 activity. Data as relative units are paired for independent experiments, n = 3, paired *t*-test based on logarithmized values.

As shown in **Figure 7**, the RMSD of the simulated protein backbone converged to equilibrium state after approximately 4 ns while **11** showed a stabilizing trend after 19 ns. As anticipated in the early simulation, the carboxylate group of **11** binds to the putative binding site by forming an important hydrogen bond with Arg52' while the prenyl group occupies the cavity at the top of the binding groove with a series of hydrophobic interactions with amino acids from helix IV (Gln134, Leu135 and Ala138) and helix I' (Tyr28' and Ile32'). The central core of **11** resides above the GSH binding site while both the phenyl rings interact with the adjacent protein hydrophobic residues (**Figure 8**). However, the carboxylate ester group of **11** failed to sustain its hydrogen bonding interaction with the guanidium side chain of Arg52' after the 19 ns mark. Without this important interaction, it is expected that **11** would possess a lower binding affinity. In contrary, the prenyl group forms a hydrophobic π-alkyl interaction with Ile25, which was evident over the entire time frames. Furthermore, the flexibility of the prenyl chain around the hydrophobic cavity could play a key role for its dual activity on both rat and human mPGES-1. This is further supported since mPGES-1 exhibits different amino acid sequence at this position resulting in a smaller edge [16].

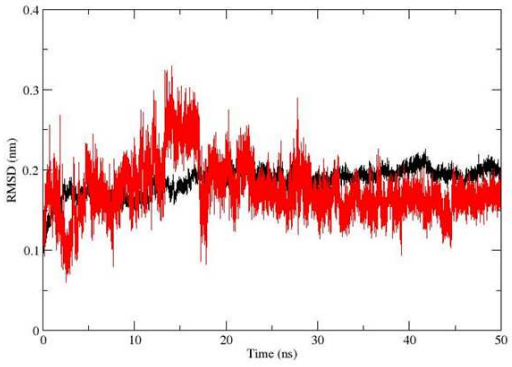

Figure 7: RMSD plots of mPGES-1 protein backbone (black line) and **11** (red line) as a function of simulation time.

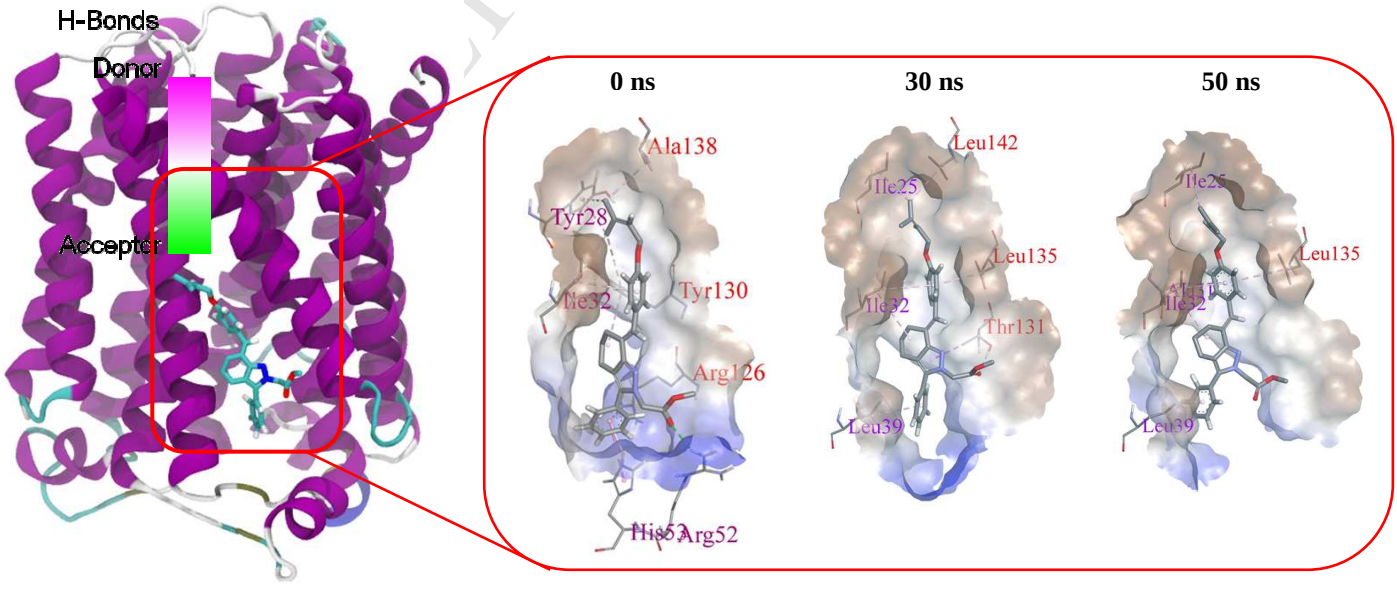

Figure 8: Binding interactions of **11** with the adjacent residues in the mPGES-1 binding site at time frame of 0 ns, 30 ns and 50 ns.

Experimental

Chemical synthesis and spectral characterizations

General procedure for the preparation of 4-((3-methylbut-2-en-1-yl)oxy)benzaldehyde ***(5).*** 10 mmol of 4-hydroxylbenzaldehyde was treated with 10 mmol of 1-chloro-3-methyl-2-butene in the presence of K_2CO_3 in acetone under reflux condition for 20 h. The reaction mixture was extracted with ethyl acetate and water, subsequently dried over anhydrous magnesium sulphate. The desired product **5** was purified by column chromatography and was used for the next steps. *General procedure for the preparation of* ***11***. A catalytic amount of *p*-toluenesulphonic acid was added into a mixture of cyclohexanone (20 mmol) and pyrrolidine (20 mmol) in 30 mL of toluene and the mixture was then refluxed on a Dean & Stark apparatus for 2 hours to prepare enamine. Upon completion, 20 mmol of benzoic anhydride in 20 mL of toluene was added dropwise into the reaction solution and stirred for 24 hours. Distilled water (10 ml) was then added and further refluxed for 30 min. The resulting reaction mixture was extracted with 3 M HCl and with 20 mL water. The toluene layer was dried over anhydrous magnesium sulphate and concentrated *in vacuo* to give crude compound. The crude compound was purified by column chromatography to afford 2-benzoylcyclohexanones. Boron trioxide (1.5 g) was added into a flask containing 10 mL of ethyl acetate in the presence of 2-benzoylcyclohexanone and stirred at 70°C for 3 hours. Compound **6** (20 mmol) and tributyl borate (20 mmol) were then added into the solution and the mixture was stirred for 30 minutes. Catalytic amount of *n*-butylamine was added dropwise and stirred for overnight followed by reflux with 10 mL of 1 M HCl for 30 minutes. The reaction mixture was extracted with ethyl acetate and dried over anhydrous magnesium sulphate. The desired product was purified by column chromatography. ***Methyl (E)-2-(7-(4-((3-methylbut-2-en-1-yl)oxy)benzylidene)-3-phenyl-4,5,6,7-tetrahydro-2H-indazol-2-yl)acetate (11).*** White crystal (32%); m.p: 114-115°C. ^{1}H NMR (600 MHz, $CDCl_3$) δ 7.73-7.74 (d, *J* = 6 Hz, 2H), 7.40-7.42 (t, *J* = 6 Hz, 2H), 7.31-7.33 (t, *J* = 6 Hz, 1H), 7.22-7.23 (d, *J* = 6 Hz, 2H), 6.91-6.93 (d, *J* = 12 Hz, 2H), 6.47 (s, 1H), 5.50-5.52 (t, *J* = 6 Hz, 1H), 5.17 (s, 2H), 4.53-4.54 (d, *J* = 6 Hz, 2H), 3.81 (s, 3H), 2.84-2.86 (m, 2H), 2.73-2.75 (m, 2H), 1.87-1.89 (m, 2H), 1.81 (s, 3H), 1.79 (s, 3H). ^{13}C NMR (151 MHz, $CDCl_3$) δ 168.97, 157.93, 148.23, 140.39, 138.42, 133.73, 130.58, 129.25, 128.56, 128.44, 127.45, 127.06, 123.83, 119.55, 116.92, 114.48, 64.84, 53.24, 52.66, 27.91, 25.85, 24.68, 22.66, 18.23.

Determination of biological activity

Cell Culture. *Murine macrophages*. The RAW264.7 cells line from the (ATCC® TIB-71™) cells line from the American Type Culture Collection (ATCC) (Manassas, VA, United States) were grown in DMEM containing 10% FBS, 1% (v/v) penicillin G/streptomycin in 5% CO_2 at 37°C. RAW264.7 cells (80–90% confluent) were detached and centrifuged at 1000 RPM at 4°C for 10 min. The viability of cultured cells used in the assay was always >95% as determined by trypan blue dye exclusion. *Cell stimulation and treatment*. RAW264.7 (5×10^5 cells/well) were seeded into a tissue culture grade 96-well plate and incubated for 24 h at 37°C, 5% CO_2 for cell attachment. The attached cells were stimulated in 100 U/mL of recombinant IFN-γ and 2 µg/mL of LPS in presence of vehicle (DMSO, 0.1%) or test compound at a final volume of 100 µL/well. Cells were then incubated at 37°C, 5% CO_2 for 17–20 h. *Cell Viability*. The cytotoxicity of test compound on cultured cells was determined by assaying the reduction of 3-(4,5-dimethylthiazol-2-yl)-2,5-diphenyl-tetrazolium bromide (MTT, 5 mg/mL in phosphate buffered saline (PBS) to formazan salts. After treatment, the supernatant were removed followed by addition of 20 µL of MTT reagents into each well. The mixture of culture media and MTT were removed after incubated at 37°C for 4 h, and the formazan salts were dissolved by adding 100% DMSO. The absorbance was then measured at 570 nm on a SpectraMax Plus microplate reader (Molecular Devices Inc., Sunnyvale, CA, USA) at room temperature.

Determination of PGE_2. The cell culture supernatants were collected and analyzed for PGE_2 secretion using PGE_2 EIA kits (Cayman Chemical, Ann Arbor, MI, USA). The protocols provided by the manufacturers were followed to the detail. The data was obtained using a SpectraMax Plus microplate reader (Molecular Device, Sunnyvale, CA, USA). The concentration of PGE_2 for each sample was calculated from their respective standard curves.

Determination of human mPGES-1 activity: Microsomes were isolated from interleukin-1β-stimulated A549 cells and mPGES-1 activity determined as previously reported [17]. In brief, microsomal membranes (2.5-5 µg total protein) were diluted in 0.1 M potassium phosphate buffer, pH 7.4, containing 2.5 mM glutathione and pre-incubated with vehicle (DMSO, 2%) or test compounds for 15 min at 4°C. PGE_2 synthesis (in a reaction volume of 100 µl) was initiated by addition of PGH_2 (20 µM final concentration) and terminated after 1 min by addition of 100 µl $FeCl_2$ (40 mM), citric acid (80 mM) and 11β-PGE_2 (10 µM) as internal standard. PGE_2 was extracted and analysed by RP-HPLC as described [17].

In silico modeling

Molecular Docking. Docking studies were performed on the crystal structure of mPGES-1 (pdb ID: 4AL1; 1.95 Å) retrieved from the Protein Data Bank using the Cdocker protocol under the receptor–ligand interaction section in Discovery Studio® 3.1 (Accelrys, San Diego, USA). Cdocker is a grid-based molecular docking method that employs CHARMM force fields. During refinement, the receptor was held rigid while the ligands were allowed to flex. High-temperature molecular dynamics, followed by random rotations, refinement by grid-based (GRID 1) simulated annealing, and a final grid-based or full force-field minimization [18] generated 200 random ligand conformations from the initial ligand structure. In this experiment, the ligand was heated to a temperature of 700 K in 2000 steps and cooled by 300 K in 5000 steps. The grid extension was set to 14 Å. Hydrogen atoms were added to the structure and all ionizable residues were set at their default protonation states at a neutral pH. The ten top ligand-binding poses were ranked according to their CDOCKER energies, and the predicted binding interactions were analyzed. The best pose was retrieved and minimized *in situ* according to the standard protocol implemented in Discovery Studio before being subjected to binding-energies and binding-scores calculations.

3D QSAR (CoMFA). To initiate the study, 29 reported MK-886 derivatives [15] that exhibited IC_{50} of less than 10 µM have been selected for *in silico* studies while 3 compounds that exhibited IC_{50} more than 10 µM have been omitted. A template-based alignment method was first applied to the molecules in the data set, in which the most active compound, i.e., **3**, was chosen as the template for the alignment of the other compounds. Nineteen compounds were categorized as the training set and the remaining ten compounds were used as the test set. The ratio of training set to test set compounds is ~7:3 and the training set

holds the most active and most inactive compounds. Similarly, the test-set compounds should cover a range of biological activities and enable evaluation of the quality of the generated 3D QSAR method. The inhibitory activity (IC_{50}) values of the studied compounds were converted into pIC_{50} using pIC_{50} = -log IC_{50} and used as dependent variables in the 3D QSAR calculations. To accelerate the analysis and reduce noise, column filtering was set at three different energies, i.e., 2.0, 1.5 and 1.0 kcal/mol, such that only the higher steric and electrostatic energies in each case were considered in the partial least-squares (PLS) analysis. The highest values of the cross-validated correlation coefficient (q^2) and non-cross-validation (r^2) were used to judge the quality of the models and avoid over-fitting. The cross-validated result quantifies the predictive ability of the model and is determined by the leave-one-out (LOO) procedure of cross-validation, in which each compound is successively removed from the model derivation. Finally, the predictive quality of the "best" correlation model was determined.

Molecular dynamics simulation. The molecular dynamics simulation input files were prepared using GROMACS v2016.3 with the united-atom GROMOS96 54a7 force field [19]. The parameterization of **11** was carried out using ATB (Automated Topology Builder) server [20]. The POPC bilipid layer membrane structure along with the Berger Lipid parameters were retrieved from Biocomputing Group website [21]. The protein-ligand complex structure was then packed with the lipids using the InflateGRO methodology. Next, the membrane protein system was solvated with water molecules. To avoid random water molecules from filling up the gaps in the lipid acyl chains, the van der Waals radii of the carbon atoms in the system were artificially enlarged by changing the value of 0.15 to 0.375. The final system contained three protein chains, 123 POPC moieties and 4545 water molecules, (a total of 24683 atoms in a 70 Å × 70 Å × 71 Å simulation box). The ionic strength was adjusted by the addition of 0.1 M of NaCl with a total of 40 Na^+ and 63 Cl^- ions. The complex was subjected to energy minimization, followed by 5 ns of NVT equilibration and 5 ns of NPT equilibration. The production run was performed using the LINCS algorithm to constrain bond lengths and periodic boundary conditions were applied in all directions [22]. Long range electrostatic forces will be treated using the Fast Particle-Mesh Ewald method (PME) [23]. Van der Waals forces and Coulomb potential were treated using a cut-off of 1.2 nm and the simulation time step was set to 2 fs. An initial velocity obtained according to a Maxwell distribution at 310 K is given to all the atoms. Nosé-Hoover thermostat and semiisotropic Parinello-Rahman pressure coupling were set at 310 K and 1 bar with a coupling time of τT = 0.5 ps and τP = 2 ps, respectively [24, 25]. The run was set for 50 ns at constant pressure and temperature conditions.

Conclusion

Compound **11** was successfully synthesized as a mPGES-1 inhibitor guided by a 3D-QSAR CoMFA approach. The compound is predicted to lack the pan-assay interference properties due to removal of the diketone linker. Apart from that, both carboxylic acid and prenyl groups have been identified to play a vital role in the activity. Future study shall address the structure-activity relationships of this novel class of mPGES-1 inhibitor in more detail.

Acknowledgement

This work was financially supported by ScienceFund (02-01-02-SF00665), Ministry of Science, Technology & Innovation, Malaysia and FRGS (FRGS/2/2014/ST01/UKM/02/3), Ministry of High Education, Malaysia. Authors also thank Universiti Kebangsaan Malaysia for the funds provided under the Research University Grant UKM-DIP-2014-16.

References

[1] C. Jegerschold, S.C. Pawelzik, P. Purhonen, P. Bhakat, K.R. Gheorghe, N. Gyobu, K. Mitsuoka, R. Morgenstern, P.J. Jakobsson, H. Hebert, Structural basis for induced formation of the inflammatory mediator prostaglandin E2, Proceedings of the National Academy of Sciences of the United States of America 105(32) (2008) 11110-5.

[2] S. Chandrasekharan, N.A. Foley, L. Jania, P. Clark, L.P. Audoly, B.H. Koller, Coupling of COX-1 to mPGES1 for prostaglandin E2 biosynthesis in the murine mammary gland, Journal of lipid research 46(12) (2005) 2636-48.

[3] H.H. Chang, E.J. Meuillet, Identification and development of mPGES-1 inhibitors: where we are at?, Future medicinal chemistry 3(15) (2011) 1909-34.

[4] C.L. Tham, C.Y. Liew, K.W. Lam, A.-S. Mohamad, M.K. Kim, Y.K. Cheah, Z.-A. Zakaria, M.-R. Sulaiman, N.H. Lajis, D.A. Israf, A synthetic curcuminoid derivative inhibits nitric oxide and proinflammatory cytokine synthesis, European Journal of Pharmacology 628(1–3) (2010) 247-254.

[5] K.-H. Lee, F.H. Ab. Aziz, A. Syahida, F. Abas, K. Shaari, D.A. Israf, N.H. Lajis, Synthesis and biological evaluation of curcumin-like diarylpentanoid analogues for anti-inflammatory, antioxidant and anti-tyrosinase activities, European Journal of Medicinal Chemistry 44(8) (2009) 3195-3200.

[6] C.L. Tham, K.W. Lam, R. Rajajendram, Y.K. Cheah, M.R. Sulaiman, N.H. Lajis, M.K. Kim, D.A. Israf, The effects of a synthetic curcuminoid analogue, 2,6-bis-(4-hydroxyl-3-methoxybenzylidine)cyclohexanone on proinflammatory signaling pathways and CLP-induced lethal sepsis in mice, European Journal of Pharmacology 652(1–3) (2011) 136-144.

[7] S.N.A. Bukhari, G. Lauro, I. Jantan, G. Bifulco, M.W. Amjad, Pharmacological evaluation and docking studies of α,β-unsaturated carbonyl based synthetic compounds as inhibitors of secretory phospholipase A2, cyclooxygenases, lipoxygenase and proinflammatory cytokines, Bioorganic & Medicinal Chemistry 22(15) (2014) 4151-4161.

[8] S. Leong, S. Faudzi, F. Abas, M. Aluwi, K. Rullah, L. Wai, M. Bahari, S. Ahmad, C. Tham, K. Shaari, N. Lajis, Synthesis and Sar Study of Diarylpentanoid Analogues as New Anti-Inflammatory Agents, Molecules 19(10) (2014) 16058.

[9] S.M. Mohd Faudzi, S.W. Leong, F. Abas, M.F.F. Mohd Aluwi, K. Rullah, K.W. Lam, S. Ahmad, C.L. Tham, K. Shaari, N.H. Lajis, Synthesis, biological evaluation and QSAR studies of diarylpentanoid analogues as potential nitric oxide inhibitors, MedChemComm 6(6) (2015) 1069-1080.

[10] S.W. Leong, S.M. Mohd Faudzi, F. Abas, M.F.F. Mohd Aluwi, K. Rullah, K.W. Lam, M.N. Abdul Bahari, S. Ahmad, C.L. Tham, K. Shaari, N.H. Lajis, Nitric oxide inhibitory activity and antioxidant evaluations of 2-benzoyl-6-benzylidenecyclohexanone analogs, a novel series of curcuminoid and diarylpentanoid derivatives, Bioorganic & Medicinal Chemistry Letters 25(16) (2015) 3330-3337.

[11] M.F.F. Mohd Aluwi, K. Rullah, B.M. Yamin, S.W. Leong, M.N. Abdul Bahari, S.J. Lim, S.M. Mohd Faudzi, J. Jalil, F. Abas, N. Mohd Fauzi, N.H. Ismail, I. Jantan, K.W. Lam, Synthesis of unsymmetrical monocarbonyl curcumin analogues with potent inhibition on prostaglandin E2 production in LPS-induced murine and human macrophages cell lines, Bioorganic & Medicinal Chemistry Letters.

[12] A. Koeberle, H. Northoff, O. Werz, Curcumin blocks prostaglandin E2 biosynthesis through direct inhibition of the microsomal prostaglandin E2 synthase-1, Mol Cancer Ther 8(8) (2009a) 2348-55.

[13] M. Iranshahi, M.G. Chini, M. Masullo, A. Sahebkar, A. Javidnia, M. Chitsazian Yazdi, C. Pergola, A. Koeberle, O. Werz, C. Pizza, S. Terracciano, S. Piacente, G. Bifulco, Can Small Chemical Modifications of Natural Pan-inhibitors Modulate the Biological

Selectivity? The Case of Curcumin Prenylated Derivatives Acting as HDAC or mPGES-1 Inhibitors, J Nat Prod 78(12) (2015) 2867-79.
[14] K. Rullah, M.F.F. Mohd Aluwi, B.M. Yamin, M.N. Abdul Bahari, L.S. Wei, S. Ahmad, F. Abas, N.H. Ismail, I. Jantan, L.K. Wai, Inhibition of prostaglandin E2 production by synthetic minor prenylated chalcones and flavonoids: Synthesis, biological activity, crystal structure, and in silico evaluation, Bioorganic & Medicinal Chemistry Letters 24(16) (2014) 3826-3834.
[15] D. Riendeau, R. Aspiotis, D. Ethier, Y. Gareau, E.L. Grimm, J. Guay, S. Guiral, H. Juteau, J.A. Mancini, N. Methot, J. Rubin, R.W. Friesen, Inhibitors of the inducible microsomal prostaglandin E2 synthase (mPGES-1) derived from MK-886, Bioorganic & medicinal chemistry letters 15(14) (2005) 3352-5.
[16] S.C. Pawelzik, N.R. Uda, L. Spahiu, C. Jegerschold, P. Stenberg, H. Hebert, R. Morgenstern, P.J. Jakobsson, Identification of key residues determining species differences in inhibitor binding of microsomal prostaglandin E synthase-1, J Biol Chem 285(38) (2010) 29254-61.
[17] A. Koeberle, U. Siemoneit, U. Buhring, H. Northoff, S. Laufer, W. Albrecht, O. Werz, Licofelone suppresses prostaglandin E2 formation by interference with the inducible microsomal prostaglandin E2 synthase-1, The Journal of pharmacology and experimental therapeutics 326(3) (2008) 975-82.
[18] G. Wu, D.H. Robertson, C.L. Brooks, 3rd, M. Vieth, Detailed analysis of grid-based molecular docking: A case study of CDOCKER-A CHARMm-based MD docking algorithm, Journal of computational chemistry 24(13) (2003) 1549-62.
[19] D. Van Der Spoel, E. Lindahl, B. Hess, G. Groenhof, A.E. Mark, H.J. Berendsen, GROMACS: fast, flexible, and free, J Comput Chem 26(16) (2005) 1701-18.
[20] A.K. Malde, L. Zuo, M. Breeze, M. Stroet, D. Poger, P.C. Nair, C. Oostenbrink, A.E. Mark, An Automated Force Field Topology Builder (ATB) and Repository: Version 1.0, Journal of Chemical Theory and Computation 7(12) (2011) 4026-4037.
[21] O. Berger, O. Edholm, F. Jähnig, Molecular dynamics simulations of a fluid bilayer of dipalmitoylphosphatidylcholine at full hydration, constant pressure, and constant temperature, Biophysical Journal 72(5) (1997) 2002-2013.
[22] B. Hess, H. Bekker, H.J.C. Berendsen, J.G.E.M. Fraaije, LINCS: A linear constraint solver for molecular simulations, Journal of Computational Chemistry 18(12) (1997) 1463-1472.
[23] T. Darden, D. York, L. Pedersen, Particle mesh Ewald: An N·log(N) method for Ewald sums in large systems, The Journal of Chemical Physics 98(12) (1993) 10089-10092.
[24] S. Nosé, A molecular dynamics method for simulations in the canonical ensemble, Molecular Physics 52(2) (1984) 255-268.
[25] M. Parrinello, A. Rahman, Crystal Structure and Pair Potentials: A Molecular-Dynamics Study, Physical Review Letters 45(14) (1980) 1196-1199.

UNIVERSITI KEBANGSAAN MALAYSIA
The National University of Malaysia

FakultiFarmasi | *Faculty of Pharmacy*

30 April 2019

Professor Jan Lundell, PhD
Editor
Journal of Molecular Structure

Dear Sir,

Submission of Manuscript Entitled 'Design and synthesis of a novel mPGES-1 lead inhibitor guided by 3D-QSAR CoMFA'

I hereby include a copy of the revised manuscript entitled 'Design and synthesis of a novel mPGES-1 lead inhibitor guided by 3D-QSAR CoMFA' for consideration to be published in your respective journal.

This paper describes the design and synthesis of unsymmetrical pyrazolocurcumin derivative as a novel mPGES-1 lead inhibitor guided by *in silico* 3D-QSAR CoMFA studies of MK-886 derivatives. The biological and computational results presented in this study will also allow the readers to understand the plausible protein-ligand complex interactions involved. We are of the opinion that the publication of this paper in your journal will provide the scientific community a wider understanding on the application of modeling studies in the field of drug discovery.

Looking forward to hearing from you.

Thank you.

Yours sincerely,

Lam Kok Wai, PhD
Drug and Herbal Research Centre
Faculty of Pharmacy
Universiti Kebangsaan Malaysia
Jalan Raja Muda Abdul Aziz
50300 Kuala Lumpur, Malaysia
Tel : +60392897031
Email: david_lam@ukm.edu.my

Highlights

- We have successfully designed and synthesized a novel mPGES-1 lead inhibitor guided by *in silico* 3D-QSAR CoMFA studies of MK-886 derivatives.
- The biological and modeling results presented provide in-depth understanding on the plausible binding interactions between **11** and mPGES-1 binding site.